The Design of Advanced Thin-film Catalysts for Electrooxidation of Formic Acid

Journal:	*ACS Catalysis*
Manuscript ID	cs-2023-055209.R1
Manuscript Type:	Article
Date Submitted by the Author:	29-Dec-2023
Complete List of Authors:	Tripkovic, Dusan; Institute of Chemistry Technology and Metallurgy, Electrochemistry Milosevic, Dragana; Institute of Chemistry Technology and Metallurgy, Ecology and Techno economics Stevanovic, Sanja; Institute of Chemistry Technology and Metallurgy, Electrochemistry Popovic, Ksenija; Institute of Chemistry Technology and Metallurgy, Electrochemistry Jovanovic, Vladislava; Univerzitet u Beogradu, ICTM Department of Electrochemistry Lopes, Pietro; Argonne National Laboratory, Material Science Department Farinazzo Bergamo Dias Martins, Pedro; University of Ljubljana Faculty of Chemistry and Chemical Technology, Stamenkovic, Vojislav; University of California Irvine, Chemical and Biomolecular Engineering; University of California Irvine, Chemical and Biomolecular Engineering Strmcnik, Dusan; National Institute of Chemistry Slovenia, Department of Materials Chemistry

The Design of Advanced Thin-film Catalysts for Electrooxidation of Formic Acid

Dušan V. Tripković[*a], Dragana L. Milošević [b], Sanja I. Stevanović [a], Ksenija Dj. Popović [a], Vladislava M. Jovanović [a], Pietro P. Lopes [c], Pedro F. B. D. Martins [d,f], Vojislav R. Stamenković [e] and Dušan Strmčnik [f]*

[a]University of Belgrade - Institute of Chemistry, Technology and Metallurgy, Department of Electrochemistry, Njegoševa 12, 11000 Belgrade, Serbia.

[b]University of Belgrade - Institute of Chemistry, Technology and Metallurgy, Department of Ecology and TechnoEconomics, Njegoševa 12, 11000 Belgrade, Serbia.

[c]Materials Science Department, Argonne National Laboratory, 9700 S Cass Ave, ZIP 60439, Lemont, IL, USA.

* Corresponding author: dusan@ihtm.bg.ac.rs (D. V. Tripković)

[d]University of Ljubljana, Faculty of Chemistry and Chemical Technology, Vecna pot 113, SI-1000 Ljubljana, Slovenia.

[e]Department of Chemical and Biomolecular Engineering, Horiba Institute for Mobility and Connectivity University of California Irvine, Irvine, CA 92697-2700.

[f]National Institute of Chemistry, SI-1000 Ljubljana, Slovenia

Abstract

Successful development of catalysts for electrochemical formic acid oxidation (FAO) requires finding an optimal balance between catalytic performance (activity/stability/selectivity) and the catalyst cost. While platinum is one of the most active catalyst materials for FAO, it suffers from performance loss at low overpotentials due to poisoning with CO, which is one of the intermediates formed in the so-called indirect path of FAO. In this work, we explored the synergistic effects of the supporting material and annealing temperature on the performance of Pt thin films for FAO in acidic media. Compared to the as-prepared Pt films, the annealed films show up to 5-fold and 15-fold improvement for FAO on Pt@Ni and Pt@Cr, respectively. While the most active Pt@Ni thin film shows the lowest stability, the most active Pt@Cr thin film is

also the most stable, challenging conventional trade-offs in electrocatalysis and providing a promising candidate for FAO nanocatalyst synthesis.

Keywords

Pt thin films; Nickel and chromium; Thermal treatment; Formic acid; Electro-oxidation

Introduction

The electrocatalytic oxidation of small organic molecules, such as methanol, ethanol and formic acid has been extensively studied due to their properties that make them suitable for use in fuel cells [1–5]. Particularly, the electrochemical oxidation of formic acid has been comprehensively examined as the anodic reaction in direct formic acid fuel cell (DFAFC) and as a model reaction important for understanding the electrooxidation of other small organic molecules. On platinum, which is one of the most active metals for formic acid oxidation (FAO), the reaction is known to proceed through a dual path mechanism. In the direct path, the reaction proceeds directly to CO_2 through an adsorbed intermediate, formate ($HCOO_{ad}$):

$$HCOOH \rightarrow CO_2 + 2H^+ + 2e^- \quad (1)$$

while in the indirect path, the poisoning CO_{ad} species are formed first, before being oxidized to CO_2 [6–12]:

$$HCOOH \rightarrow COad + H_2O \rightarrow CO_2 + 2H^+ + 2e^- \quad (2)$$

The main goal in the development of the catalysts for FAO is to find the optimal balance between catalytic performance (activity/stability/selectivity) and the catalyst cost, i.e. quantity of the noble metal used [6,13–15]. However, platinum and its alloys, which are among the best catalysts for FAO, are particularly susceptible to poisoning species which significantly reduces their catalytic performance at low potentials [16, 17]. Several strategies are in place to mitigate this issue, such as tuning the catalyst's selectivity by surface modification with a second metal, tuning its activity by changing the electronic properties via alloying with transition metals as well as tuning the selectivity/activity through catalyst's surface morphology (facet dependent catalytic properties).

An additional approach is the tuning of catalysts properties through the introduction of electrochemically stable support material [18]. Interactions between deposited metal and supports are of crucial importance and can significantly affect the performance of the catalyst. The electronic, geometric and bifunctional effects originating from strong metal-support interactions

(SMSI) can determine the essential catalyst properties such as activity, selectivity, and stability [19–22]. In conjunction with thermal annealing, this approach also enables the rearrangement of surface atoms, and therefore, can significantly alter the structure of Pt surfaces, including the prospect of alloying with the support [23, 24].

Here, we present the thin film approach in the design of an advanced electrocatalyst for formic acid oxidation through the utilization of nickel and chromium supports and thermal treatment. In general, among the numerous methods for synthesis, thin film based catalysts obtained by deposition of a noble metal over geometrically defined non-noble metallic substrate serves as a link between well-defined extended single crystalline surfaces and high surface area nanoscale catalysts. Moreover, these systems provide the guideline for real-world catalyst design by effective utilization and transfer of critical physical properties into the catalyst's structure [25–28]. Specifically, for the two different substrates, Ni and Cr, the selective combination of customized electroanalytical methods, thermal annealing in the controlled environment, atomic force microscopy (AFM), specific adsorption of Bi, including electrooxidation of adsorbed carbon monoxide layer were used to reveal the insight into the structure-function relationship for Pt-thin film catalyst. While annealed Pt@Ni and Pt@Cr show significant improvement, 5-fold and 15-

fold, in electrocatalytic activity compared to the as-prepared surfaces the mechanism of improvement is very different. Moreover, the selectivity and stability of explored surfaces were found to be critically different, with Pt@Cr annealed surface having the most desirable enhancement of both, which is opposite to commonly observed activity-stability tradeoffs in electrocatalysis [29, 30].

Experimental

Electrode preparation

High purity Ni and Cr discs, 6 mm diameter, were used as the substrate for all thin film electrodepositions. Prior to each experiment, Ni and Cr electrodes were mirror polished using silicon carbide grinding paper (Buehler, P800 - P4000) and 1-0.05 μm alumina (Buehler). The surface was then rinsed with high purity water and sonicated for 2-3 min. Before each electrodeposition of platinum, a cyclic voltammogram of pure Ni or Cr electrode was recorded (potential range 0.05 V to 1.25 V vs RHE, sweep rate 50 mV s^{-1}) in 0.1 M $HClO_4$ solution, to ensure that the surface was clean and electrochemically treated.

Platinum was electrochemically deposited on Ni or Cr substrate under potentiostatic conditions in deoxygenated 0.1 M $HClO_4$ + 1 mM H_2PtCl_6 solution. The deposition was carried out in three consecutive steps, from an initial potential hold at 0.05 V vs RHE for 2 s to a final potential of 0.07 V vs. RHE during 50 s. The amount of platinum was estimated from integrated charge measured from the *i-t* transient response corrected for metal (Ni or Cr, M in further text) substrate charging. This method produces stable Pt thin films with a thickness of around 100 atomic monolayers (ML), which is approximately 25 nm. After the deposition, the as-prepared Pt@M electrode was cycled in the potential between hydrogen and oxygen regions (0.05 V to 1.25 V vs RHE) until reaching a stable voltammogram and then annealed in the reductive atmosphere (95% Ar+5% H_2) [31] at selected temperature, either 300 °C or 500 °C for 2 hours.

Characterization of the catalysts

Surface characterization of the catalysts was performed at room temperature in the air by atomic force microscopy using a NanoScope III D (Veeco, USA) instrument. The AFM

measurements were carried out in the taping mode using silicon nitride cantilevers with a force constant of 0.06 N m^{-1}. Analysis of all surfaces, based on AFM images, was done by selecting 5 different parts of the sample (500x500nm). The measurements of the mean surface island size and size distribution were acquired from a few randomly chosen areas in the AFM images containing about 100 individual islands. AFM measurements were made before and after thermal treatments.

Electrochemical measurements

The rotating disk electrode (RDE) measurements were carried out in 0.1 M $HClO_4$ solution at the room temperature in a standard three electrodes/three compartment glass cell. The Pt wire and bridged saturated calomel electrode (SCE) were used as counter and reference electrodes, respectively. The electrolytes used were prepared with high purity water ("Millipore", 18.2 MΩ cm resistivity) and p.a. grade chemicals ("Merck"). All solutions were pre-saturated with nitrogen and kept with the inert atmosphere for the duration of the experiments.

After the deposition of Pt onto the M substrate, the electrodes were thoroughly rinsed with high purity water and transferred to the cell containing 0.1 M $HClO_4$. The electrochemically active surface area of Pt@M electrodes used was estimated from the integrated charge in hydrogen adsorption/desorption region (potential range from 0.05 V to 0.45 V) and CO_{ad} stripping curve with a correction for a double layer charging, from the steady-state cyclic voltammograms in the supporting electrolyte, assuming a charge of 210 μC/cm^2 for a monolayer of adsorbed hydrogen, and 420 μC/cm^2 for a monolayer of adsorbed CO.

The electrocatalytic activity of Pt@M electrodes for formic acid oxidation was tested in 0.1 M $HClO_4$ solution containing 0.5 M HCOOH ("Merck"), which was added to the supporting electrolyte while holding the electrode potential at 0.05 V. The potential was cycled at a sweep rate of 50 mV s^{-1}. The relevant information on (111) ordered domains on Pt@M samples were obtained from the specific and selective irreversible adsorption of Bi. The detailed procedure was given elsewhere. [32, 33]

In-situ FTIR measurments

All IR measurements were performed in a spectroelectrochemical glass cell designed for an external reflection mode in a thin layer configuration in 0.1 M $HClO_4$ solution containing 0.5 M HCOOH. The cell is coupled at its bottom with a CaF_2 prism beveled at 60˚ from the prism base. Nicolet Nexus 670 spectrometer, equipped with a liquid-N_2 cooled MCT detector was used. The spectra were recorded with a resolution of 8 cm^{-1}. All measurements were performed using p-polarized light.

Stability measurements

To evaluate the stability of the Pt@M against dissolution and deactivation due to potential cycling the custom built RDE setup in conjunction with inductively coupled plasma mass spectrometry (ICP-MS) was used. The *in situ* ICP-MS experiments were done using the stationary probe rotating disk electrode (SPRDE) system coupled to an ICP-MS (Perkin Elmer) as described elsewhere in the literature [34]. These experiments were carried out in a blank 0.1 M $HClO_4$ electrolyte.

Results and Discussion

Catalyst surface characterization

The AFM images of the Pt thin film deposited over Ni and Cr show the difference in the morphology (Figure 1a and Figure 2a). This implies that the nature of the substrate can dictate the Pt deposition which results in the different surface morphology. The AFM images of as prepared and annealed Ni and Cr substrates are given in Supplementary Information (SI) (Figure S1).

Pt@Ni surface:

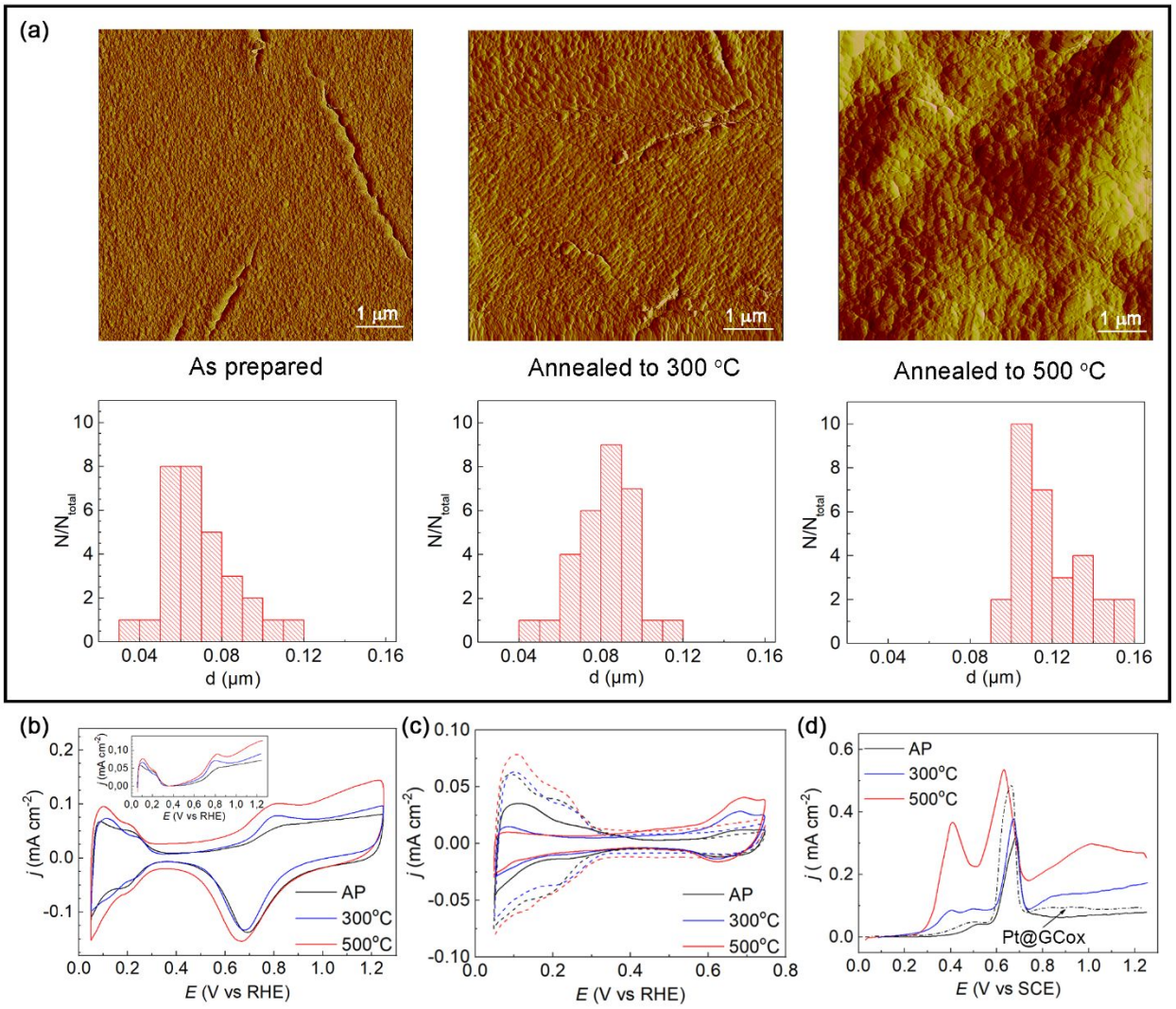

Figure 1. **(a)** AFM images (5x5 microns) and corresponding surface islands size distributions for Pt@Ni catalyst; **(b)** Voltammograms and positive-going scans after double layer subtraction (inset) for Pt@Ni catalyst; **(c)** Voltammetric profile of the Pt@Ni electrode covered with irreversibly adsorbed bismuth. The dashed line corresponds to the baseline used for the charge measurement. **(d)** CO stripping curves of Pt@Ni catalyst (black dotted line - as prepared

Pt@GCox); Black curves -as prepared, blue curves - annealed to 300 °C, and red curves - annealed to 500 °C. Test solution 0.1 M $HClO_4$; sweep rate: 50 mV s^{-1}.

Figure 1a shows the surface morphology of differently treated Pt@Ni electrodes revealed by AFM. As prepared Pt@Ni electrode consists of predominantly spherical particles, with an average size of 60 nm, fairly uniform distribution and high surface coverage. Upon annealing, the particle growth is observed first on Pt@Ni at 300 °C, while at 500 °C, the average particle size becomes approximately 120 nm. In addition, surface roughening can also be observed with the increase of annealing temperature, and is the most evident at 500 °C. Close inspection of the cyclic voltammogram for as prepared Pt film on Ni substrate resembles polycrystalline platinum. Consistent with the observed roughening, the voltammograms in Figure 1b exhibit a change in shape in the underpotentially deposited hydrogen (H_{UPD}) region, (0.05 V < E < 0.4 V) as well as in the region of surface oxide formation, (0.45 V < E < 1.25 V).

Apart from the observation that the thermal annealing is inducing the change in the ratio of specific surface structures due to the rearrangement of the surface atoms, it is difficult to discern from the voltammogram alone, how the annealing is affecting the ratios of individual crystal planes on the surface. A much better tool to achieve that is the structure sensitive selective

adsorption of Bi (Figure 1c). This method, which was demonstrated to be a convenient surface specific method for determining the Pt surface structures [32, 33, 35], shows an increase of Pt(111) terrace site fraction from 8% on as prepared to 48% for the annealed Pt@Ni at 500 °C (Table 1).

Finally, we note that annealing seems to cause the migration of some of the Ni from the underlying substrate to the surface. This can be concluded from the CO stripping experiments in Figure 1d, where an additional peak can be seen appearing at 0.4 V with the annealing. This peak is usually associated with the oxidation of CO on Ni sites [36, 37] and is absent on the as prepared Pt@Ni surface, which looks very similar to the response obtained on Pt deposited on glassy carbon (Pt@GC) or Cr substrate (Pt@Cr), figure 1(d). Due to the partial removal of adsorbed CO_{ad} on surface Ni from the annealed Pt@Ni catalyst, the CO stripping peak on Pt is shifted to more negative potentials, in contrast with the expected positive shift due to the increasing fraction of Pt(111) domains in the film.

Pt@Cr surface:

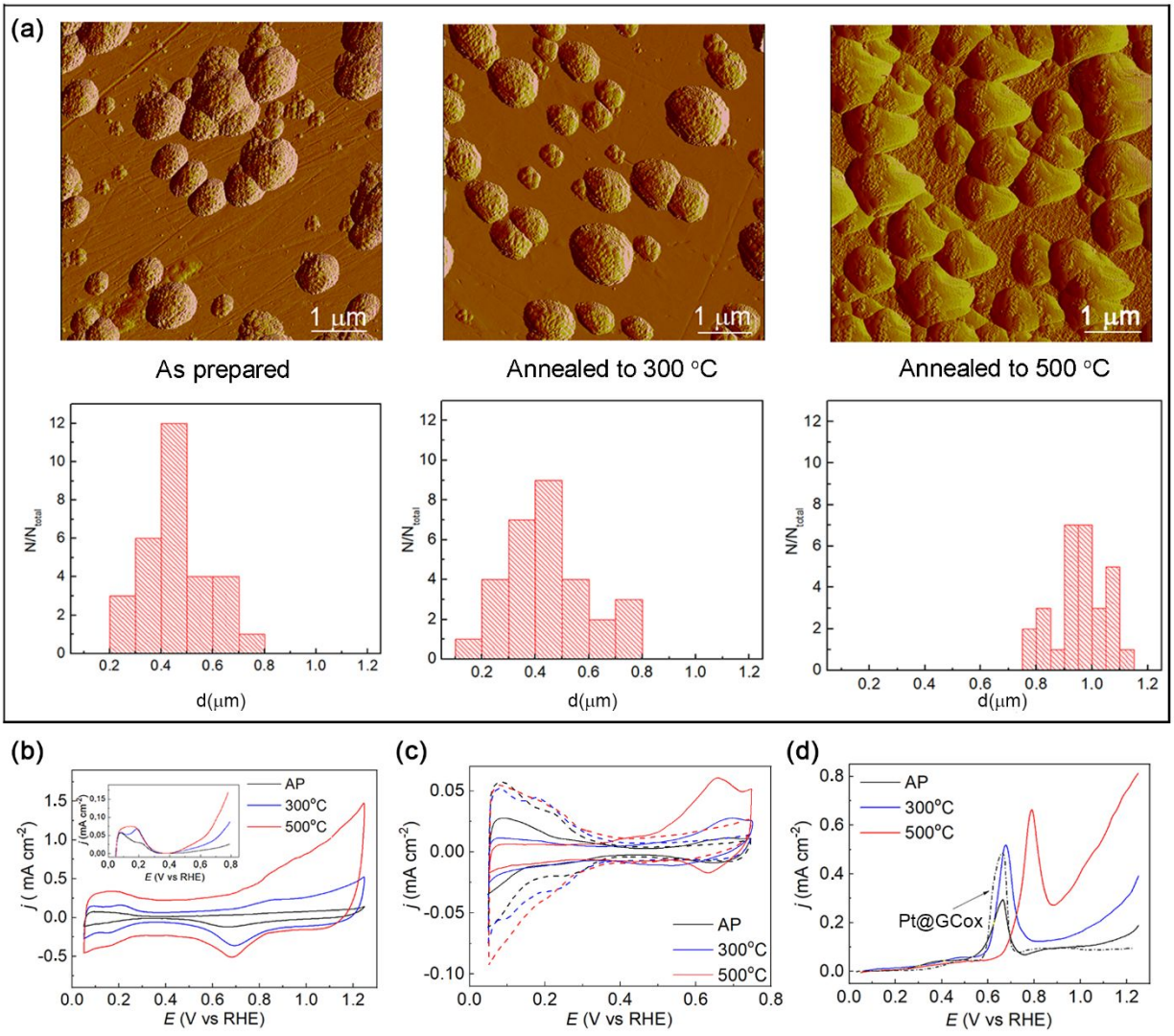

Figure 2. **(a)** AFM images (5x5 microns) and corresponding surface islands size distributions for Pt@Cr catalyst; **(b)** Voltammograms and positive-going scans after double layer subtraction (inset) for Pt@Cr catalyst; **(c)** Voltammetric profile of the Pt@Cr electrode covered with irreversibly adsorbed bismuth. The dashed line corresponds to the baseline used for the charge measurement. **(d)** CO stripping curves of Pt@Cr catalyst (black dotted line - as prepared

Pt@GC_{ox}); Black curves -as prepared, blue curves - annealed to 300 °C and red curves - annealed to 500 °C. Test solution 0.1 M $HClO_4$; sweep rate: 50 mV s^{-1}.

In contrast to the Pt@Ni surface, the as prepared Pt@Cr electrode (Figure 2a) has predominantly large, spherically shaped Pt islands, with wider size distribution and much lower surface coverage compared to the Pt@Ni. With annealing, the islands increase in diameter from an average of 0.45 μm for the as prepared surface to 1 μm for the annealed surface at 500 °C. Most notably, the islands also change their morphology at higher annealing temperatures (500 °C), becoming more flat and faceted. In the voltammograms (Figure 2b), that is manifested in the H_{UPD} region with an increase of the peak current at 0.3 V, usually associated with (111)x(100) surface sites [38]. At 500 °C, the H_{UPD} area becomes completely flat, resembling the Pt(111) voltammogram. Both Bi adsorption as well as CO stripping results are also well aligned with this conclusion. The fraction of (111) domains increases from 9% for the as prepared compared to 81% for the 500 °C annealed surface (Figure 2c and Table 1).

The CO stripping peak in Figure 2d shifts towards more positive potentials with the increase in annealing temperature, which is indicative of restructuring towards (111) surface, consistent with the trend for CO stripping peak potential on platinum single: Pt(110) < Pt(100) < Pt(111) [39, 40].

Table 1. Fraction of the (111) ordered domains determined for as-prepared and annealed Pt@Ni and Pt@Cr electrodes.

Sample	Pt@Ni	Pt@Cr
as-prepared	8.0%	8.6%
annealed 300 °C	24%	40%
annealed 500 °C	48%	81%

After electrochemical and AFM surface structure evaluations, the activity of these catalysts for formic acid oxidation reaction as well as their stability and selectivity were determined.

Formic acid oxidation

The performance of the Pt low-index single crystals was evaluated first in order to establish the basis for the understanding of the role of the surface structure on the FOA activity, selectivity and stability of different surface structures during formic acid oxidation. The characteristic signatures observed for each crystalline structure are given in Figure 3. The dual path mechanism of the FAO, the direct [41, 6] and indirect, both produce CO_2 as the final reaction product, nevertheless, they proceed at very different potentials. At low potentials from 0.35 to 0.75 V, which is relevant for formic acid fuel cell operation, the FOA specific activity exhibits the following trend: Pt(111)>Pt(100)>Pt(110), as shown in Figure 3. As abundantly explained in the literature [9], this trend is based on the selectivity towards the direct reaction pathway, which avoids the formation of poisoning CO_{ad} species. In fact, the simultaneous formation of CO at low potentials on steps and defects is the main cause of the lower activity of Pt(110) and Pt(100) compared to Pt(111). After the removal of CO_{ad} through electrooxidation, which is facilitated by adsorbed oxygenated species at higher potentials (0.75-1.15V), the reverse trend of activity occurs Pt(110)>Pt(100)>Pt(111) [42, 43]. The height of the oxidation peak in the positive potential region is an indication of the degree of Pt poisoning at lower potentials [43]. Overall, Pt single crystalline surfaces reveal the cause of structure sensitivity for the catalytic activity of the FAO,

which is related to preventing the formation of CO or its removal from the surface, either through the direct reaction pathway or the formation of oxygenated surface species, respectively. Finally, we note that these Pt single crystalline surfaces display negligible dissolution at potentials below 0.5 V [44].

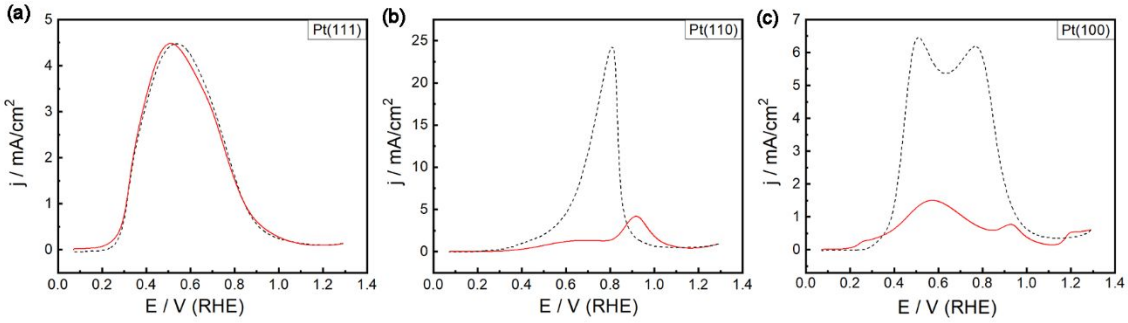

Figure 3. Voltammograms for electrooxidation of 0.5 M HCOOH in 0.1 M $HClO_4$ on **(a)** Pt(111), **(b)** Pt(110) and **(c)** Pt(100) surfaces; positive scan direction - red solid line and negative scan direction - gray dotted line.

Next, we have analyzed the electrochemical behavior of Pt@Ni and Pt@Cr thin film catalysts. The polarization curves and corresponding activities at 0.35V for HCOOH oxidation on differently treated Pt@Ni and Pt@Cr electrodes are summarized in Figure 4.

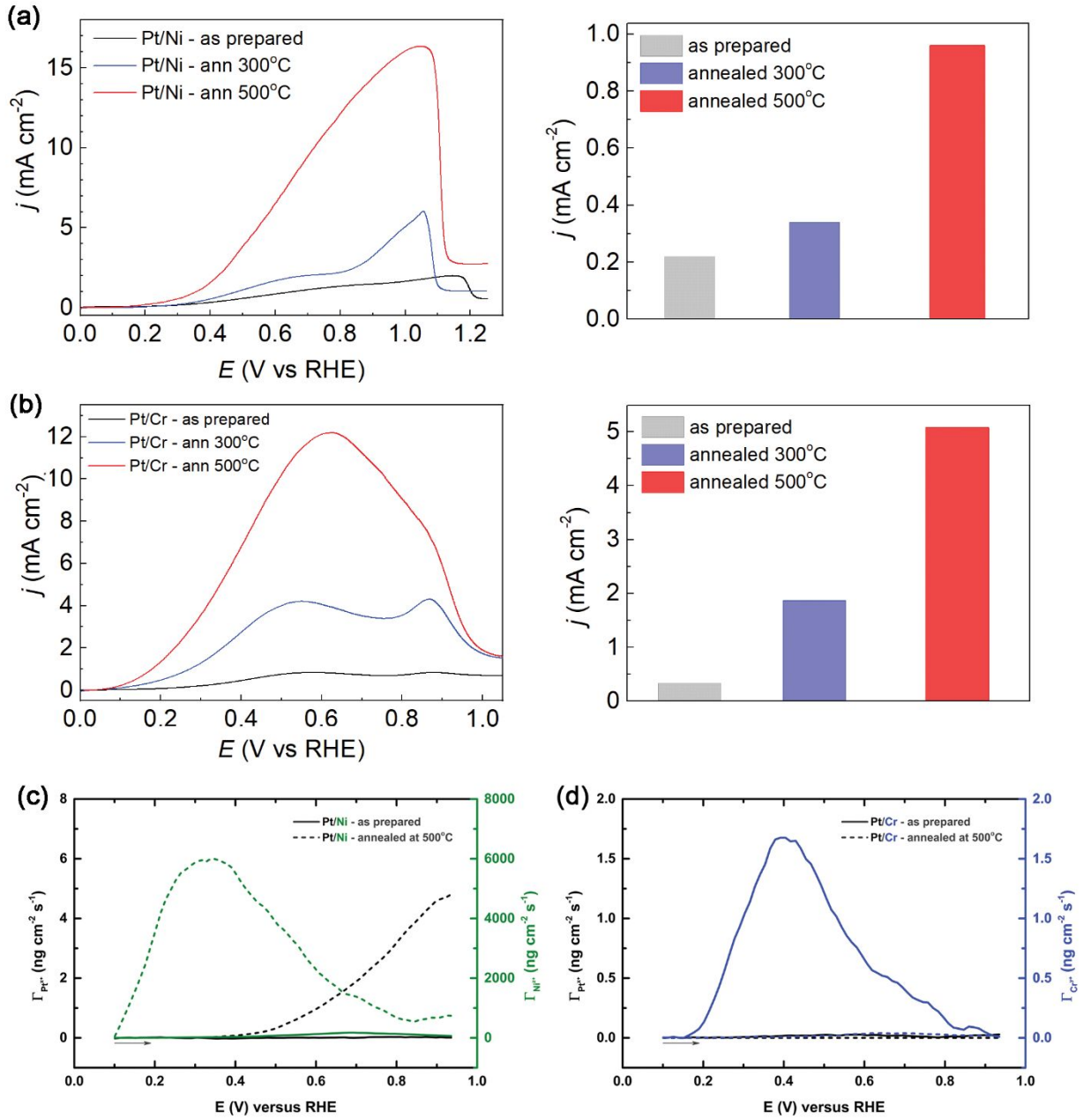

Figure 4. Polarization curves in anodic sweep and corresponding activity obtained at 0.35 V for electrooxidation of 0.5 M HCOOH in 0.1 M $HClO_4$ on (a) Pt@Ni and (b) Pt@Cr surfaces and in situ ICP-MS dissolution of Pt@Ni (c) and Pt@Cr (d) surfaces: As prepared-solid line and annealed to 500 °C-dashed line.

Note that all voltammograms for oxidation of formic acid were found to be insensitive to the rotation of the electrode, indicating that the reaction is still under kinetic control within the entire potential region. Anodic and cathodic scans are given in (SI) (Figure S2).

The voltammogram of the as-prepared Pt@Ni electrode (Figure 4a) shows distinct similarities with Pt (110) surface, typical for polycrystalline samples, with two broad peaks/plateaus centered between 0.25-0.85 V and 0.85-1.15 V. Upon annealing, both peaks show a substantial increase in current density as well as a shift towards negative potential, reaching the maximum activity at 500 °C. Compared to the as-prepared surface, or Pt (110), the activation at 0.35 V is roughly 5-fold. However, the effect seems to be much more pronounced on the more positive peak, which dominates the overall electrochemical response. The observed activation for the FAO, based on the CO stripping experiments, is attributed to the effect of Ni present on the surface. With the improved ability of the surface to remove the adsorbed CO, formed during FAO, the Pt@Ni surface is becoming more active for the indirect reaction path. It should be mentioned that the increased presence of (111) sites, determined by Bi_{UPD} method, can also contribute to the activity increase via direct path. Nevertheless, the relative fraction of 48% is not enough to sustain the activity at low potentials without the assistance of CO-removal by oxygenated species.

Similar to the Pt@Ni surface, the voltammogram of the as-prepared Pt@Cr electrode (Figure 4b-black curve) resembles that of Pt (110), with the reaction proceeding through both paths presented by two anodic peaks of almost equal activity. However, the changes after annealing the Pt@Cr electrode to 300 and 500 ^{o}C are quite different than in the case of Pt@Ni. In contrast to the Pt@Ni electrode, the first process, associated with the direct path, is prevalent, resulting in a bell-shaped curve, which is typical for Pt (111) single crystal electrode (Figure 3a). The specific activity increase is almost 15-fold compared to the as-prepared surface and 2-fold compared to Pt (111). We attribute such activity boost to the thermal treatment-induced surface reconstruction in favor of (111) orientation and full segregation of Pt over Cr. This is in good agreement with the observations obtained by AFM, voltammetry and Bi_{UPD}, which confirmed a dramatic increase in the fraction of Pt (111) facets. Nevertheless, it was important to confirm that the FAO was indeed proceeding through the direct oxidation of HCOOH to CO_2, without significant formation of CO_{ad} poisoning species. In situ FTIR analysis has revealed that Pt@Cr surface annealed at 500 ^{o}C (Supplementary Information Figure S3 (3d)) does not have CO_{ad} peak at any potential during the electrooxidation of formic acid, which implies that the reaction proceeds without the formation of CO_{ad}, i.e., the same way as on Pt(111), (Supplementary Information: Figure S3

(3b)). These results confirm a significant activity increase on both substrates upon annealing, as well as the selectivity increase towards the direct FOA mechanism on Pt@Cr.

To complete the performance characterization of our supported thin films, we performed stability testing of annealed and as-prepared surfaces during FAO by SPRDE-ICP-MS. The Pt-like stability of as-prepared Pt@Ni surface, with essentially no dissolution of Pt or Ni at potentials below 0.75 V vs. RHE (Figure 4c), suggests that the deposited Pt film on Ni is dense, non-porous. Upon annealing, which significantly increases the activity of the surface, a massive dissolution of both Pt and Ni was detected already at potentials around -0.35 V. Again, the explanation for the observed effect is indicated by the CO stripping experiments (Figure 1d), which show that a substantial amount of Ni seems to migrate to the surface upon annealing, causing an extensive dissolution of Ni in the acidic environment as well as making the adjacent Pt more prone to degradation. This is in line with the so-called inverse activity-stability relationship, which postulates that there is a tradeoff between the activity and stability of electrocatalytic materials. In rare examples, though, an inverse of this relationship is observed. We find that our annealed Pt@Cr system falls into that category. The as-prepared Pt@Cr catalyst shows signs of significant dissolution of Cr substrate, while Pt film is stable at potentials below

0.75 V vs. RHE, which is a direct consequence of the island-like film morphology, leaving substantial portions of the Cr exposed. Interestingly, the annealing of the Pt@Cr sample caused, in addition to the 15-fold activation at 0.15 V RHE, also two orders of magnitude lower dissolution of Cr at the same potential, as well as additional stabilization of Pt film. We attribute the stabilization of Pt to a higher fraction of the inherently more stable (111) facets in the annealed sample, while the origin of the Cr stability seems to be some sort of passivation during annealing, most likely by trace oxygen in the annealing gas (SI) (Figure S4). Nonetheless, the 500 ^{o}C annealed Pt@Cr catalyst was found to be the most active, the most selective and the most stable catalyst in our study. A catalyst with the best marks for all three characteristics is a very rare find in electrocatalysis in general.

Conclusion

In the work presented herein, we explored the synergistic effects of the supporting material and annealing temperature on the performance of Pt thin film catalysts for formic acid electrooxidation in acidic media. Our results show that compared to the as-prepared Pt films, the

annealed (500 °C) Pt@Ni and Pt@Cr films show exceptional activity for FAO reaction, with 5-fold and 15-fold improvement, respectively.

On annealed Pt@Ni, the activation is a consequence of the bifunctional effect, i.e. formic acid is oxidized predominantly on platinum through the indirect pathway forming CO in the process, while the poisoning CO_{ad} is oxidized on adjacent Ni, that has migrated to the surface during annealing, resulting in improved activity. However, the increase in activity leads to enhanced instability of the thin-film catalyst, and a significant dissolution of both Pt and Ni is observed in the relevant potential window, in line with the often-observed activity-stability relationship.

In contrast, the improved activity on annealed Pt@Cr system is a consequence of the surface reconstruction of Pt film with predominant (111) orientation. Compared to other facets, the (111) facet selectively favors direct HCOOH oxidation, avoiding CO_{ad} poisoning and thus higher activity at low potentials. Moreover, the Pt (111) facets offer improved stability of the catalyst compared to the as-prepared polycrystalline film. Finally, the Cr substrate also experiences improved stability after annealing, presumably due to the formation of a protective oxide layer. Thus, with the successful choice of the supporting material and annealing temperature, we were

able to create a thin film catalyst with improved activity, selectivity and stability, which is quite rare in electrocatalysis.

Author Contributions

D. Tripković conceptualized this work, wrote the original manuscript draft and performed in-depth data analysis. D. Milosević drew the visualizations and performed image editing. S. Stevanović performed the AFM measurements. K. Popović has carried out the Bi adsorption experiments and manuscript draft revision. V. Jovanović done the manuscript revison. P. Lopes and P. Martins have carried out the ICP-MS measurments. V. Stamenković performed final review & editing of the manuscript. D. Stmčnik analyzed the data and co-wrote the paper. .

Acknowledgment

This research was funded by the Ministry of Science, Technological Development and Innovation of the Republic of Serbia (contract No 451-03-47/2023-01/200026) and by the

Science Fund of the Republic of Serbia under grant No 7739802. D. Strmcnik and P.F.B.D Martins would like to acknowledge the Slovenian Research and Innovation Agency (ARIS) program P2–0393 and project J7-4636.

References

(1) Parsons, R.; VanderNoot, T. The Oxidation of Small Organic Molecules. A Survey of Recent Fuel Cell Related Research. *J. Electroanal. Chem.* **1988**, *257* (1–2), 9–45. https://doi.org/10.1016/0022-0728(88)87028-1.

(2) Jarvi, T.; Stuve, E. Fundamental Aspects of Vacuum and Electrocatalytic Reactions of Methanol and Formic Acid on Platinum Surfaces. *Electrocatalysis* **1998**, 75.

(3) Reitz, W. Handbook of Fuel Cells: Fundamentals, Technology, and Applications, (Volume 2) W. Vielstich, A. Lamm, and H. A. Gasteiger (Editors). *Mater. Manuf. Process.* **2007**, *22* (6), 789–789. https://doi.org/10.1080/10426910701416336.

(4) Marković, N. M.; Ross, P. N. Surface Science Studies of Model Fuel Cell Electrocatalysts.

Surf. Sci. Rep. **2002**, *45* (4–6), 117–229. https://doi.org/10.1016/s0167-5729(01)00022-x.

(5) Jiang, K.; Zhang, H. X.; Zou, S.; Cai, W. Bin. Electrocatalysis of Formic Acid on Palladium and Platinum Surfaces: From Fundamental Mechanisms to Fuel Cell Applications. *Phys. Chem. Chem. Phys.* **2014**, *16* (38), 20360–20376. https://doi.org/10.1039/c4cp03151b.

(6) Capon, A.; Parsons, R. The Oxidation of Formic Acid at Noble Metal Electrodes Part III. Intermediates and Mechanism on Platinum Electrodes. *J. Electroanal. Chem.* **1973**, *45* (2), 205–231. https://doi.org/10.1016/S0022-0728(73)80158-5.

(7) Iwasita, T.; Xia, X.; Herrero, E.; Liess, H. D. Early Stages during the Oxidation of HCOOH on Single-Crystal Pt Electrodes as Characterized by Infrared Spectroscopy. *Langmuir* **1996**, *12* (17), 4260–4265. https://doi.org/10.1021/la960264s.

(8) Herrero, E.; Feliu, J. M. Understanding Formic Acid Oxidation Mechanism on Platinum Single Crystal Electrodes. *Curr. Opin. Electrochem.* **2018**, *9*, 145–150. https://doi.org/10.1016/j.coelec.2018.03.010.

(9) Boronat-González, A.; Herrero, E.; Feliu, J. M. Heterogeneous Electrocatalysis of Formic

Acid Oxidation on Platinum Single Crystal Electrodes. *Curr. Opin. Electrochem.* **2017**, *4* (1), 26–31. https://doi.org/10.1016/j.coelec.2017.06.003.

(10) Cuesta, A.; Cabello, G.; Osawa, M.; Gutiérrez, C. Mechanism of the Electrocatalytic Oxidation of Formic Acid on Metals. *ACS Catal.* **2012**, *2* (5), 728–738. https://doi.org/10.1021/cs200661z.

(11) Ferre-Vilaplana, A.; Perales-Rondón, J. V.; Buso-Rogero, C.; Feliu, J. M.; Herrero, E. Formic Acid Oxidation on Platinum Electrodes: A Detailed Mechanism Supported by Experiments and Calculations on Well-Defined Surfaces. *J. Mater. Chem. A* **2017**, *5* (41), 21773–21784. https://doi.org/10.1039/c7ta07116g.

(12) Xu, J.; Yuan, D.; Yang, F.; Mei, D.; Zhang, Z.; Chen, Y. X. On the Mechanism of the Direct Pathway for Formic Acid Oxidation at a Pt(111) Electrode. *Phys. Chem. Chem. Phys.* **2013**, *15* (12), 4367–4376. https://doi.org/10.1039/c3cp44074e.

(13) Rice, C.; Ha, S.; Masel, R. I.; Wieckowski, A. Catalysts for Direct Formic Acid Fuel Cells. *J. Power Sources* **2003**, *115* (2), 229–235. https://doi.org/10.1016/S0378-7753(03)00026-0.

(14) Yu, X.; Pickup, P. G. Recent Advances in Direct Formic Acid Fuel Cells (DFAFC). *J. Power Sources* **2008**, *182* (1), 124–132. https://doi.org/10.1016/j.jpowsour.2008.03.075.

(15) Jiang, J.; Kucernak, A. Nanostructured Platinum as an Electrocatalyst for the Electrooxidation of Formic Acid. *J. Electroanal. Chem.* **2002**, *520* (1–2), 64–70. https://doi.org/10.1016/S0022-0728(01)00739-2.

(16) Park, S.; Xie, Y.; Weaver, M. J. Electrocatalytic Pathways on Carbon-Supported Platinum Nanoparticles: Comparison of Particle-Size-Dependent Rates of Methanol, Formic Acid, and Formaldehyde Electrooxidation. *Langmuir* **2002**, *18* (15), 5792–5798. https://doi.org/10.1021/la0200459.

(17) Wang, X.; Hu, J. M.; Hsing, I. M. Electrochemical Investigation of Formic Acid Electro-Oxidation and Its Crossover through a Nafion ® Membrane. *J. Electroanal. Chem.* **2004**, *562* (1), 73–80. https://doi.org/10.1016/j.jelechem.2003.08.010.

(18) Samjeské, G.; Miki, A.; Ye, S.; Osawa, M. Mechanistic Study of Electrocatalytic Oxidation of Formic Acid at Platinum in Acidic Solution by Time-Resolved Surface-Enhanced Infrared Absorption Spectroscopy. *J. Phys. Chem. B* **2006**, *110* (33), 16559–

16566. https://doi.org/10.1021/jp0618911.

(19) Wang, Y. J.; Wilkinson, D. P.; Zhang, J. Noncarbon Support Materials for Polymer Electrolyte Membrane Fuel Cell Electrocatalysts. *Chem. Rev.* **2011**, *111* (12), 7625–7651. https://doi.org/10.1021/cr100060r.

(20) Maillard, F.; Bonnefont, A.; Micoud, F. An EC-FTIR Study on the Catalytic Role of Pt in Carbon Corrosion. *Electrochem. commun.* **2011**, *13* (10), 1109–1111. https://doi.org/10.1016/j.elecom.2011.07.011.

(21) Cerri, I.; Nagami, T.; Davies, J.; Mormiche, C.; Vecoven, A.; Hayden, B. Innovative Catalyst Supports to Address Fuel Cell Stack Durability. *Int. J. Hydrogen Energy* **2013**, *38* (1), 640–645. https://doi.org/10.1016/j.ijhydene.2012.06.089.

(22) Fu, Q.; Wagner, T. Interaction of Nanostructured Metal Overlayers with Oxide Surfaces. *Surf. Sci. Rep.* **2007**, *62* (11), 431–498. https://doi.org/10.1016/j.surfrep.2007.07.001.

(23) Pan, C. J.; Tsai, M. C.; Su, W. N.; Rick, J.; Akalework, N. G.; Agegnehu, A. K.; Cheng, S. Y.; Hwang, B. J. Tuning/Exploiting Strong Metal-Support Interaction (SMSI) in Heterogeneous Catalysis. *J. Taiwan Inst. Chem. Eng.* **2017**, *74*, 154–186.

https://doi.org/10.1016/j.jtice.2017.02.012.

(24) Su, Y.; Liu, H.; Yan, Z.; Feng, M.; Tang, J.; Du, H. Platinum Nanowires: Structural and Catalytic Evolution upon Annealing Temperature. *Electrochim. Acta* **2015**, *164*, 182–186. https://doi.org/10.1016/j.electacta.2015.02.126.

(25) Chung, D. Y.; Chung, Y. H.; Jung, N.; Choi, K. H.; Sung, Y. E. Correlation between Platinum Nanoparticle Surface Rearrangement Induced by Heat Treatment and Activity for an Oxygen Reduction Reaction. *Phys. Chem. Chem. Phys.* **2013**, *15* (32), 13658–13663. https://doi.org/10.1039/c3cp51520f.

(26) Snyder, J.; Danilovic, N.; Paulikas, A. P.; Tripkovic, D.; Strmcnik, D.; Markovic, N. M.; Stamenkovic, V. R. Thin Film Approach to Single Crystalline Electrochemistry. *J. Phys. Chem. C* **2013**, *117* (45), 23790–23796. https://doi.org/10.1021/jp4078272.

(27) Snyder, J.; Markovic, N. M.; Stamenkovic, V. R. Single Crystalline Thin Films as a Novel Class of Electrocatalysts. *J. Serbian Chem. Soc.* **2013**, *78* (11), 1689–1702. https://doi.org/10.2298/JSC130916119S.

(28) Van Der Vliet, D. F.; Wang, C.; Tripkovic, D.; Strmcnik, D.; Zhang, X. F.; Debe, M. K.;

Atanasoski, R. T.; Markovic, N. M.; Stamenkovic, V. R. Mesostructured Thin Films as Electrocatalysts with Tunable Composition and Surface Morphology. *Nat. Mater.* **2012**, *11* (12), 1051–1058. https://doi.org/10.1038/nmat3457.

(29) Beermann, V.; Gocyla, M.; Kühl, S.; Padgett, E.; Schmies, H.; Goerlin, M.; Erini, N.; Shviro, M.; Heggen, M.; Dunin-Borkowski, R. E.; Muller, D. A.; Strasser, P. Tuning the Electrocatalytic Oxygen Reduction Reaction Activity and Stability of Shape-Controlled Pt-Ni Nanoparticles by Thermal Annealing -Elucidating the Surface Atomic Structural and Compositional Changes. *J. Am. Chem. Soc.* **2017**, *139* (46), 16536–16547. https://doi.org/10.1021/jacs.7b06846.

(30) Hanief, N.; Lang, C. I.; Bucher, R.; Topic, M. Phase Transformations and Surface Characterization of the Platinumchromium Coated System. *J. South. African Inst. Min. Metall.* **2012**, *112* (7), 501–504.

(31) Tripković, D. V.; Popović, K. D.; Jovanović, V. M.; Nogueira, J. A.; Varela, H.; Lopes, P. P.; Strmcnik, D.; Stamenkovic, V. R.; Markovic, N. M. Tuning of Catalytic Properties for Electrooxidation of Small Organic Molecules on Pt-Based Thin Films via Controlled

Thermal Treatment. *J. Catal.* **2019**, *371*, 96–105. https://doi.org/10.1016/j.jcat.2019.01.038.

(32) A, E. S. S.; Clavilier, J.; Feliu, J. M.; Aldaz, A. An Irreversible Struci'ure Sensitive Adsorption Bismuth Undeizpotential Deposition at Platinum Eleci-Rodes Step In. **1988**, *243*, 419–433.

(33) Rodríguez, P.; Herrero, E.; Solla-Gullón, J.; Vidal-Iglesias, F. J.; Aldaz, A.; Feliu, J. M. Specific Surface Reactions for Identification of Platinum Surface Domains: Surface Characterization and Electrocatalytic Tests. *Electrochim. Acta* **2005**, *50* (21), 4308–4317. https://doi.org/10.1016/j.electacta.2005.02.087.

(34) Lopes, P. P.; Strmcnik, D.; Tripkovic, D.; Connell, J. G.; Stamenkovic, V.; Markovic, N. M. Relationships between Atomic Level Surface Structure and Stability/Activity of Platinum Surface Atoms in Aqueous Environments. *ACS Catal.* **2016**, *6* (4), 2536–2544. https://doi.org/10.1021/acscatal.5b02920.

(35) Devivaraprasad, R.; Kar, T.; Chakraborty, A.; Singh, R. K.; Neergat, M. Reconstruction and Dissolution of Shape-Controlled Pt Nanoparticles in Acidic Electrolytes. *Phys. Chem.*

Chem. Phys. **2016**, *18* (16), 11220–11232. https://doi.org/10.1039/c5cp07832f.

(36) Chen, Y.; Shi, J.; Chen, S. Small Molecule (CO, H2) Electro Oxidation as an Electrochemical Tool for Characterization of Ni@Pt/C with Different Pt Coverages. *J. Phys. Chem. C* **2015**, *119* (13), 7138–7145. https://doi.org/10.1021/jp512283c.

(37) Chung, Y. H.; Chung, D. Y.; Jung, N.; Park, H. Y.; Yoo, S. J.; Jang, J. H.; Sung, Y. E. Origin of the Enhanced Electrocatalysis for Thermally Controlled Nanostructure of Bimetallic Nanoparticles. *J. Phys. Chem. C* **2014**, *118* (19), 9939–9945. https://doi.org/10.1021/jp5019982.

(38) Koper, M. T. M. Structure Sensitivity and Nanoscale Effects in Electrocatalysis. *Nanoscale* **2011**, *3* (5), 2054–2073. https://doi.org/10.1039/c0nr00857e.

(39) García, G.; Koper, M. T. M. Stripping Voltammetry of Carbon Monoxide Oxidation on Stepped Platinum Single-Crystal Electrodes in Alkaline Solution. *Phys. Chem. Chem. Phys.* **2008**, *10* (25), 3802–3811. https://doi.org/10.1039/b803503m.

(40) Yang, Y.; Agarwal, R. G.; Hutchison, P.; Rizo, R.; Soudackov, A. V.; Lu, X.; Herrero, E.; Feliu, J. M.; Hammes-Schiffer, S.; Mayer, J. M.; Abruña, H. D. Inverse Kinetic Isotope

Effects in the Oxygen Reduction Reaction at Platinum Single Crystals. *Nat. Chem.* **2023**, *15* (2), 271–277. https://doi.org/10.1038/s41557-022-01084-y.

(41) Cuesta, A.; Cabello, G.; Gutiérrez, C.; Osawa, M. Adsorbed Formate: The Key Intermediate in the Oxidation of Formic Acid on Platinum Electrodes. *Phys. Chem. Chem. Phys.* **2011**, *13* (45), 20091–20095. https://doi.org/10.1039/c1cp22498k.

(42) Adžić, R. R.; Tripković, A. V.; Vešović, V. B. Structural Effects in Electrocatalysis: Oxidation of Formic Acid and Hydrogen Adsorption on Platinum Single-Crystal Stepped Surfaces. *J. Electroanal. Chem.* **1986**, *204* (1–2), 329–341. https://doi.org/10.1016/0022-0728(86)80530-7.

(43) Grozovski, V.; Climent, V.; Herrero, E.; Feliu, J. M. Intrinsic Activity and Poisoning Rate for HCOOH Oxidation on Platinum Stepped Surfaces. *Phys. Chem. Chem. Phys.* **2010**, *12* (31), 8822–8831. https://doi.org/10.1039/b925472b.

(44) Lopes, P. P.; Li, D.; Lv, H.; Wang, C.; Tripkovic, D.; Zhu, Y.; Schimmenti, R.; Daimon, H.; Kang, Y.; Snyder, J.; Becknell, N.; More, K. L.; Strmcnik, D.; Markovic, N. M.; Mavrikakis, M.; Stamenkovic, V. R. Eliminating Dissolution of Platinum-Based

Electrocatalysts at the Atomic Scale. *Nat. Mater.* **2020**, *19* (11), 1207–1214. https://doi.org/10.1038/s41563-020-0735-3.

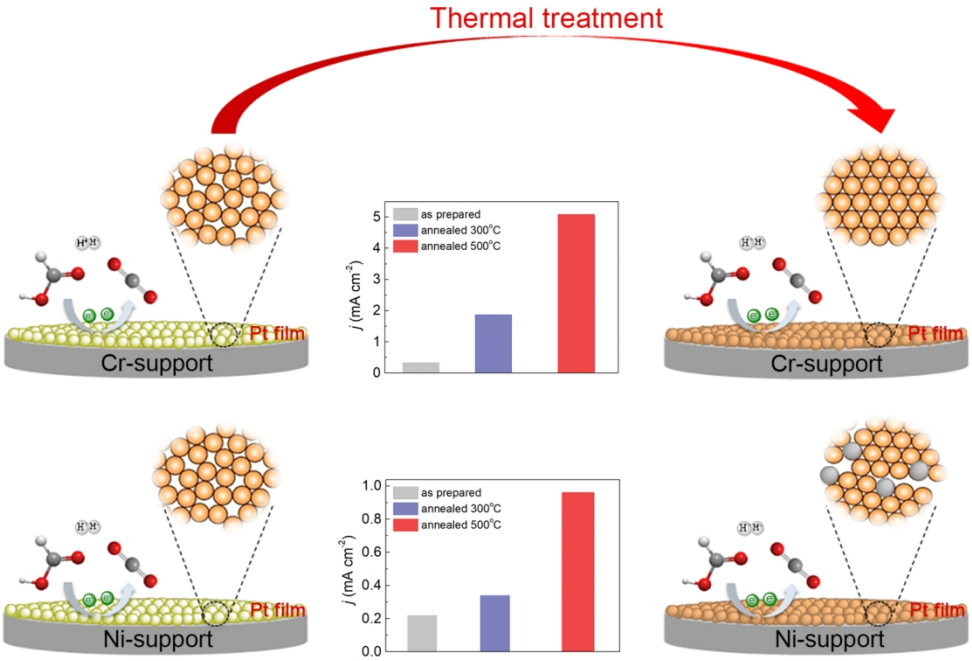

150x102mm (300 x 300 DPI)